RSC Medicinal Chemistry

ROYAL SOCIETY OF CHEMISTRY

RESEARCH ARTICLE

View Article Online
View Journal | View Issue

Cite this: *RSC Med. Chem.*, 2025, **16**, 312

Human microbiome derived synthetic antimicrobial peptides with activity against Gram-negative, Gram-positive, and antibiotic resistant bacteria†

Walaa K. Mousa,‡*[acd] Ashif Y. Shaikh,‡[b] Rose Ghemrawi,[ac] Mohammed Aldulaimi,[b] Aya Al Ali,[ac] Nour Sammani,[ac] Mostafa Khair,[e] Mohamed I. Helal,[f] Farah Al-Marzooq[g] and Emilia Oueis *[bh]

Received 23rd May 2024,
Accepted 9th October 2024

DOI: 10.1039/d4md00383g

rsc.li/medchem

The prevalence of antibacterial resistance has become one of the major health threats of modern times, requiring the development of novel antibacterials. Antimicrobial peptides are a promising source of antibiotic candidates, mostly requiring further optimization to enhance druggability. In this study, a series of new antimicrobial peptides derived from lactomodulin, a human microbiome natural peptide, was designed, synthesized, and biologically evaluated. Within the most active region of the parent peptide, linear peptide **LM6** with the sequence LSKISGGIGPLVIPV-NH_2 and its cyclic derivatives **LM13a** and **LM13b** showed strong antibacterial activity against Gram-positive bacteria, including resistant strains, and Gram-negative bacteria. The peptides were found to have a rapid onset of bactericidal activity and transmission electron microscopy clearly shows the disintegration of the cell membrane, suggesting a membrane-targeting mode of action.

Introduction

The high occurrence of antibiotic resistance in bacterial infections is a serious global health problem, contributing to financial burden, increased morbidity, and the death of millions worldwide.[1–3] Hence, there is an urgent need for novel antibiotics capable of targeting difficult to treat infections. One natural source of potential drugs that can be explored for antibiotics discovery is the human microbiome.[4–6] Indeed, there has been mounting evidence regarding the role that the human microbiota plays in invading pathogens, among others.[7,8] Specifically, antimicrobial peptides (AMPs), innate to all living organisms, have been shown to have a dual action as antimicrobials and modulators of the host immune system.[9,10] Natural AMPs and their derivatives show great potential as promising antibiotic candidates, notably because of their ability to penetrate bacterial cell membranes. As such, many have already been marketed as antibiotics (*i.e.* daptomycin, polymyxin B, and colistin), while others are in the clinical pipeline.[11,12] Microbiota-derived AMPs have been found to have 35 to 57 amino acids on average, with the most common producers in the gut being *Bacillus* and *Lactobacillus*.[13] In our previous work, we identified lactomodulin (LM), a class IIb bacteriocin AMP that we isolated from a strain of *Lacticaseibacillus rhamnosus* (ATCC 7469).[14] LM is a 52 amino acid long peptide belonging to the lactobin A/cerein 7B family. Our investigation into the activity of LM revealed that the peptide possesses a dual antibacterial and anti-inflammatory activity, including against resistant strains, while showing low cytotoxicity on human cell lines. In this work, we set out to find the shorter sequences derived from LM that conserve the antibacterial activity, setting the groundwork for further modifications and fine-tuning of the structural and physicochemical properties. AMPs with longer sequences

[a] *College of Pharmacy, Al Ain University, PO BOX 64141, Abu Dhabi, United Arab Emirates. E-mail: walaa.mousa@aau.ac.ae*
[b] *Department of chemistry, Khalifa University of Science and Technology, PO BOX 127788, Abu Dhabi, United Arab Emirates. E-mail: emilia.oueis@ku.ac.ae*
[c] *AAU Health and Biomedical Research Center, Al Ain University, PO BOX 112612, Abu Dhabi, United Arab Emirates*
[d] *College of Pharmacy, Mansoura University, Mansoura 35516, Egypt*
[e] *Core Technology Platforms, New York University Abu Dhabi, PO BOX 127788, United Arab Emirates*
[f] *Electron Microscopy Core Labs, Khalifa University of Science and Technology, PO BOX 127788, Abu Dhabi, United Arab Emirates*
[g] *Department of Medical Microbiology and Immunology, College of Medicine and Health Sciences, UAE University, P.O. Box 15551, Al Ain, United Arab Emirates*
[h] *Healthcare Engineering Innovation Group, Khalifa University of Science and Technology, PO BOX 127788, Abu Dhabi, United Arab Emirates*
† Electronic supplementary information (ESI) available. See DOI: **https://doi.org/10.1039/d4md00383g**
‡ These authors contributed equally to this work.

generally have unfavourable properties that hinder their therapeutic applications, including stability and cost. As such, it is important to determine the essential regions within the peptide that have functionality, or in this case antibacterial effect. The identification of these key regions is the first step in the design and development of potent antibacterial peptides with desirable properties through chemical modifications. Using systemic and rational design, a first series of nine peptides (**LM1–LM9**) derived from LM was assessed, followed by another set of five peptides (**LM10–LM13**) based on **LM6**. Compared with the parent peptide, the best analogues showed similar activity against Gram-positive pathogens, while showing additional, albite lower, Gram-negative activity *in vitro*, leading to the identification of the core key regions responsible for the antibacterial activity of LM. Killing kinetics combined with transmission electron microscopy imaging (TEM) suggested that these antimicrobial peptides might target the cell membrane resulting in its disruption in a fast-killing mode. However, this action is associated with a considerable cytotoxicity on human cell lines which needs to be addressed in the next design stage to improve the peptides' therapeutic potential.

Results and discussion

Peptide design

A library of nine short peptides derived from LM was designed and synthesized with the aim to pinpoint the pharmacophore region within the parent peptide that would retain the antibacterial activity. As such two methodologies were used generating two separate series. The first series included five peptides that were systematically derived from the primary sequence of LM by splicing it into one 12-mer (**LM1**) and four 10-mer (**LM2–LM5**) peptides (Fig. 1). The rationale behind this strategy was to cover all parts of the original AMP, regardless of any predictions. The second series consisted of four derivatives that were rationally designed through the analysis of the LM sequence, by examining and evaluating the antimicrobial prediction scores, toxicity, and secondary structure (**LM6–LM9**, Fig. 1 and Table 1). *In silico* AMP prediction tools have proven beneficial to AMP discovery and design, saving in time and cost. CAMPR3, a curated database of known AMPs, offers an AMP prediction tool based on four different prediction models: discriminant analysis (DA), support vector network (SVM), artificial neural network (ANN), and random forest (RF).[15] The latter has been shown to be the most accurate in a recent study.[16] As the aim was to generate shorter bioactive peptides, four chain length peptides (7, 10, 12, and 15-mers) were generated through the prediction tool. By overlapping the prediction results based on all four algorithms and four lengths, it was apparent that most peptides were concentrated within the K3-L30 region of LM. All the peptides were predicted to be not toxic using the ToxinPred tool based on the SVM (Swiss-Prot) and motif based method.[17] The helical secondary structure is considered as an important

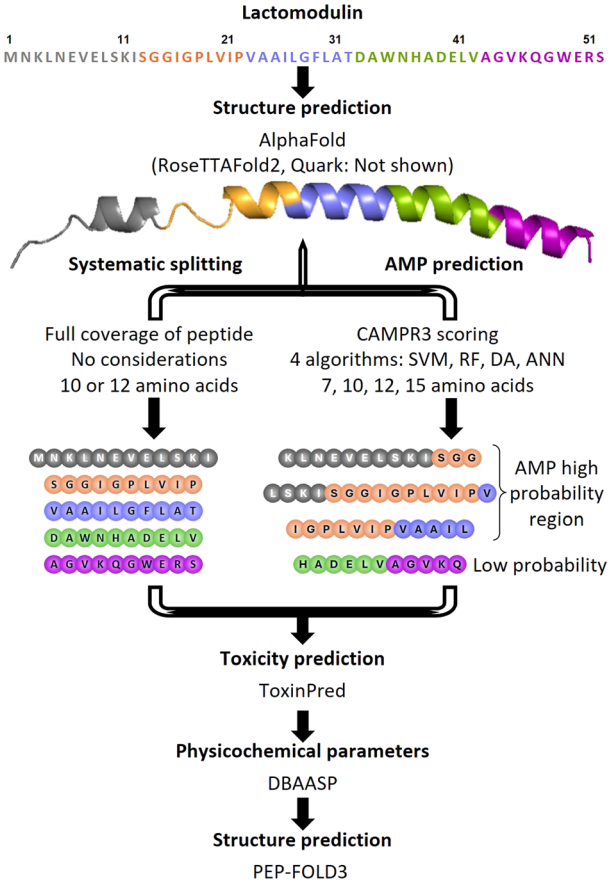

Fig. 1 Summary of the overall workflow used for the design stage.

and prominent feature of AMPs and shorter sequences within the helical region of LM would be prioritized. However, the secondary structure of LM is not known. When we used the different structure prediction tools, AlphaFold, RoseTTAFold2, and Quark for the prediction of the secondary structure of the LM peptide, there was a convergence in the results, which showed the mostly helical structure of LM (Fig. S1†). This indicates that most predicted sequences were likely to come from helical regions within LM.[18–21] Based on these results, three overlapping peptides (**LM6–LM8**) within the K3-L30 region with high AMP probability prediction were shortlisted for testing. **LM6**, a 15-mer with the sequence LSKISGGIGPLVIPV (position 9–23), along with its shorter derivatives, was one of the few peptides predicted by all four algorithms to have AMP character with high probability, occupying the centre of the AMP region. **LM7**, a 12-mer with the sequence IGPLVIPVAAIL (position 16–27), and its different variations have high scores in the RF algorithm and nicely overlap with **LM6**. **LM8**, a 13-mer with the sequence KLNEVELSKISGG (position 3–15), overlaps with **LM6** on the N-terminal side and completes the AMP predicted region. The C-terminal region of LM has low AMP probability throughout all algorithms, but the sequence HADELVAGVKQ (**LM9**) was added to the series regardless, especially as it was predicted by PEP-FOLD3 (Fig. S1†) to have an α-helical structure.[22]

Table 1 Sequences and key physicochemical parameters of the synthesized short peptides

Peptides		Characterization				Computed physicochemical properties					
Code	Sequence	Purity[a] (%)	t_R[b] (min)	Theoretical $[M + H]^+$	Measured[c] $[M + H]^+$	q[d]	P/N[e]	<H>[d]	<mH>[d]	A index[d]	*In vitro* aggregation[d]
LM	MNKLNEVELSKISGGIGPLVIPVAAILG FLATDAWNHADELVAGVKQGWERS					−2	0.93	−0.22	0.23	0.68	690.00
LM1	MNKLNEVELSKI-NH_2	76	11.81	1416.7888	1416.7736	+1	1.40	0.08	0.24	0.82	0
LM2	SGGIGPLVIP-NH_2	99	13.82	908.5569	908.5530	+1	0.67	−0.64	0.10	0	0
LM3	VAAILGFLAT-NH_2	96	14.90	974.6039	974.6000	+1	0.25	−0.81	0.22	0	589.22
LM4	DAWNHADELV-NH_2	97	15.95	1168.5387	1168.5317	−2	1.00	−0.05	0.52	0.96	0
LM5	AGVKQGWERS-NH_2	99	6.41	1116.5909	1116.5793	+2	2.33	0.23	0.40	1.56	0
LM6	LSKISGGIGPLVIPV-NH_2	98	14.51	1449.9045	1449.9154	+2	0.67	−0.55	0.34	0.24	0
LM7	IGPLVIPVAAIL-NH_2	97	15.83	1174.7927	1174.7838	+1	0.09	−0.86	0.26	0	342.26
LM8	KLNEVELSKISGG-NH_2	98	14.98	1372.7800	1372.7774	+1	2.25	0.01	0.17	0.76	0
LM9	HADELVAGVKQ-NH_2	95	9.41	1165.6329	1165.6275	0	1.20	−0.05	0.40	0.69	18.52
LM10	LSKISGGIGP-NH_2	96	13.63	927.5627	927.5567	+2	1.50	−0.35	0.39	0.37	0
LM11	KISGGIGPLV-NH_2	97	17.32	939.5991	939.5936	+2	1.00	−0.48	0.41	0.37	0
LM12	LSKISG-NH_2	95	9.94	603.3830	603.3814	+2	2.00	−0.18	0.46	0.61	0
LM13a	Cyc(LSKISGGIGPLVIPv)	95	17.76	1431.8934	1431.8874	+1	0.67				
LM13b	Cyc(LSKISGGIGPLVIPV)	95	18.35	1431.8934	1431.8874	+1	0.67				

[a] Purity as determined by analytical RP-HPLC with UV absorption at 220 nm. [b] Retention time determined by analytical RP-HPLC. [c] Protonated mass confirmed by high resolution mass spectrometry. [d] Theoretical values of the physicochemical parameters determined by DBAASP q: net charge, <H>: normalized hydrophobicity, <mH>: normalized hydrophobic moment, A index: amphiphilicity index. [e] Ratio of polar (including glycine) to non-polar amino acids.

Along with it, **LM1**, **LM3**, **LM5**, and **LM8** all showed predicted helicity as well. **LM7** is mostly a random coil, except for a four amino acid stretch (PVAA) that is helical. **LM6** is predicted to be a random coil, while the shorter version peptide **LM2** is predicted to have a β-hairpin structure with a two-residue turn (GP). Some physicochemical properties were theoretically determined using the Database of Antimicrobial Activity and Structure of Peptides (DBAASP v3.0) to assess the hydrophobicity, amphiphilicity, and toxicity of the shortlisted compounds, using the Eisenberg and Weiss hydrophobicity scale.[23,24] The parent peptide LM is negatively charged overall with a −2 charge, while the majority of known antimicrobial peptides are cationic. Anionic AMPs bind to metal ions and form salt bridges with the negatively charged bacterial membrane, allowing the AMP to penetrate through.[25] Positively charged AMPs on the other hand interact directly with the bacterial membrane. The synthesized peptides of the first library are mostly cationic (+1 or +2), except for peptides **LM4** (−2) and **LM9** (0). The peptides were synthesized as their C-terminal amide, neutralizing the carboxylic acid and securing an additional positive charge for the linear peptide. At the same time, hydrophobicity is an important characteristic of peptides, which is essential for their interaction with the hydrophobic core of bacterial membranes, and has been shown to correlate with their antibacterial activity.[26,27] An increased hydrophobicity however has been linked to hemotoxicity (red blood cell destruction). Hence, amphipathicity or amphiphilicity is important, and can be measured through the normalized hydrophobic moment. The normalized hydrophobicity of all truncated peptides and the parent peptide ranges from −0.86 to 0.23 and the normalized hydrophobic moment from 0.10 to 0.52 (Table 1). The values are within the expected ranges of known AMPs. The amphiphilicity index indicates the helical structural stability at the membrane–water interface. A value of zero shows no stability, while a higher value indicates a higher stability.[28] Three peptides showed an amphiphilicity index of zero, **LM2**, **LM3**, and **LM7**, while all the others showed a certain stability with the highest value being for **LM5**. *In vitro* aggregation propensity is a useful prediction as it is associated with lower antimicrobial activity, decreased physical stability, and increased cytotoxicity of the peptide.[29] Peptide **LM3** showed a high value, similar to the parent peptide LM (690 and 580, respectively), **LM9** showed a low propensity to *in vitro* aggregation, and all the other peptides are not predicted to aggregate.

Biological evaluation

To assess whether the synthetized peptides retained the antibiotic activity of the parent compound, we first performed an agar diffusion on a panel of human pathogens, with peptide concentration ranging from 1 to 10 μM. All the peptides showed some level of antibiotic activity. We then measured their corresponding minimum inhibitory concentration (MIC) values (Table 2), as the average of five replicates each, against a collection of Gram-positive and Gram-negative pathogens. The parent peptide LM has shown good antibacterial activity against Gram-positive pathogens *Staphylococcus aureus* ATCC 25923 (hereafter referred to as SA; 0.8 μM MIC), *Clostridium difficile* ATCC 43602 (hereafter referred to as *C. diff*; 1.1 μM MIC), and *Listeria monocytogenes*

Table 2 Antimicrobial and anti-inflammatory activities and cytotoxicity of the synthesized peptides

	MICs (μM)								Pro-inflammatory biomarker reduction (%)				EC_{50} (μM)	
	Gram-positive bacteria			Gram-positive resistant strains		Gram-negative bacteria								
Peptide	*S. aureus* ATCC 25923	*C. difficile* ATCC 43602	*L. monocytogenes* ATCC 15313	*S. aureus* MRSA BAA 2313	*E. faecium* VRE BAA 2317	*E. coli* ATCC 33694	*P. aeruginosa* BAA 1744	*S. enterica* ATCC 13314	IL-8	IL-6	IL-1B	TNF alpha	H292	A549
LM	0.8	1.1	1.2	1.4	1.2	7.5	NA	NA	95	90	91	80	—	—
LM1	6.2	NA	3.1	NA	NA	NA	NA	NA	1	2	0	0	—	—
LM2	2.1	1.6	1.2	NA	NA	8.9	9.5	NA	6	6	20	0	2.97	6.35
LM3	6.5	NA	NA	NA	NA	NA	NA	NA	0	0	0	0	—	—
LM4	2.6	NA	NA	3.5	NA	NA	NA	NA	61	50	19	0	—	—
LM5	1.2	2.1	1.8	1.4	1.9	7.8	NA	NA	18	12	18	0	2.28	11.11
LM6	0.9	0.9	2.3	1.7	1.3	9.2	9.3	NA	10	0	7	10	2.80	3.69
LM7	1.5	1.8	3.6	1.8	1.5	NA	NA	NA	18	25	27	25	—	—
LM8	2.3	2.6	2.6	2.9	3.2	NA	NA	NA	17	5	8	0	—	—
LM9	1.3	1.0	1.1	2.5	3.1	NA	NA	NA	12	32	33	40	2.72	11.71
LM10	2.4	4.1	3.7	NA	NA	NA	NA	NA	0	0	0	0	—	—
LM11	5.1	NA	NA	NA	NA	NA	NA	NA	0	0	0	0	—	—
LM12	3.9	4.6	5.1	NA	NA	NA	NA	NA	0	0	0	0	—	—
LM13a	0.8	0.9	1.5	1.7	1.5	8.2	8.3	NA	14	9	4	15	2.07	8.50
LM13b	0.7	0.9	1.5	1.6	1.8	8	8.5	NA	10	4	13	5	2.55	4.73
Amoxycillin	5	5	5	35	35	NT	NT	NT						
Fidaxomicin	NT	1	1	NT	2	NT	NT	NT						
Ciprofloxacin	2	NT	2	2	4	2	2	2						

NA: not observed within the tested concentrations. NT: not tested on these strains.

ATCC 15313 (hereafter referred to as Lm; 1.2 μM MIC), as well as the resistant strains: methicillin resistant *Staphylococcus aureus* BAA 2313 (hereafter referred to as MRSA; 1.4 μM MIC) and vancomycin resistant *Enterococcus faecium* BAA 2317 (hereafter referred to as VRE; 1.2 μM MIC). It also showed low activity against the Gram-negative *Escherichia coli* ATCC 33694 (hereafter referred to as *E. coli*; 1.2 μM MIC), while no activity was observed at the highest tested concentration against the other Gram-negatives *Pseudomonas aeruginosa* BAA 1744 and *Salmonella enterica* ATCC 13314 (hereafter referred to Pa and Sen, respectively). The least active peptide of the first series is **LM3**, followed by **LM1**. **LM3** is only active against SA with an MIC of 6.5 μM. It has a high hydrophobicity and a high propensity for *in vitro* aggregation. **LM4** is the only peptide with a total negative charge and has the highest normalized hydrophobic moment with a high amphiphilicity index. In terms of activity however, the peptide showed MICs only against SA and MRSA, at 2.6 μM and 3.5 μM, respectively. **LM2** showed activity against the Gram-positive pathogens SA, *C. diff*, and Lm with acceptable MIC values compared to LM, that is 2.1 μM, 1.6 μM, and 1.2 μM, respectively. However, it showed no activity at the tested concentration against the drug resistant strains. On the other hand, it showed activity against *E. coli* with an MIC of 8.9 μM in the same range as the parent peptide. More interestingly, **LM2** showed a new activity against the Gram-negative strain Pa, with an MIC of 9.5 μM. Its physicochemical properties show a normalized hydrophobicity and normalized hydrophobic moment of −0.64 and 0.10, respectively, with an amphiphilicity index of zero, indicating an instability of the helical structure at the membrane–water interface. The last peptide of the systemic splicing is **LM5** at the C-terminal of LM. It is positively charged with a +2 charge, has a high ratio of polar amino acids, and has the highest hydrophobicity of the family. It also shows high stability of its helical structure. **LM5** showed good MIC values within the same range as the parent peptide against all Gram-positive pathogens (MIC SA = 1.2 μM, *C. diff.* = 2.1 μM, Lm = 1.8 μM), including resistant strains (MIC MRSA = 1.4 μM and VRE = 1.9 μM), as well as *E. coli* (MIC = 7.8 μM). Looking at the correlation between the antibacterial activity of the peptides and their physicochemical properties, it seems non-existent. The peptides coming from the different regions within LM are very different in terms of their primary sequence, hence making the comparison of their properties quite difficult, especially that the predicted values are well within the range of what is expected for AMPs. Regardless, just by focusing on the bioactivity profile of these systematically truncated peptides, we could identify two potential areas that can be further exploited and that showed the better activities, **LM2** and **LM5**.

The activity of the rationally designed peptides by looking mostly at their AMP prediction also correlates with these results. Very similar in primary structure to **LM1**, **LM8** has most of the amino acids of **LM1** except MN from the N-terminal with the additional SGG at the C-terminal. Most of its predicted physicochemical properties are similar or within the same range as **LM1**. The only difference is the ratio of polar to non-polar residue. But conversely, **LM8** has a much better activity profile against all Gram-positive pathogens with MICs in the range of 2.3 μM to 3.2 μM, including resistant strains (2.9 μM and 3.2 μM). However, **LM8** was the weakest compound within this second series. **LM7** is a hybrid between **LM2** and **LM3** and has shown improvement in its MIC value compared to them against SA (1.5 μM), while recovering the activity against the resistant strains MRSA (1.8 μM) and VRE (1.5 μM). It was less active nonetheless against *C. diff.* (1.8 μM) and Lm (3.6 μM). However, it remained inactive against the Gram-negative pathogens. **LM7** is highly hydrophobic and is predicted to aggregate *in vitro*. **LM6**, the peptide at the core of the AMP prediction region, showed a very good activity profile, almost matching the parent peptide activity with only 15 amino acids. The MIC against SA is 0.9 μM and 1.7 μM against MRSA, 0.9 μM against *C. diff.*, 2.3 μM against Lm, and 1.3 μM against VRE. The Gram-negative *E. coli* activity is also conserved with an MIC of 9.2 μM, while a new Pa activity was also introduced with 9.3 μM MIC. Most peptides performed better than amoxycillin against the Gram-positive bacteria, and in particular activity was observed against resistant strains. Similar activity to fidaxomicin was observed for the most active peptides (**LM6** and **LM9**) against *C. diff*, while the others were slightly less active. More specifically, the activity of **LM6** is superior to both ciprofloxacin and amoxycillin in inhibiting Gram-positive bacteria while comparable to fidaxomicin in killing *C. difficile* (Table 2). However, it is about 5 times less active than ciprofloxacin against the Gram-negative bacteria. **LM6** is the best peptide of the series and the library. When looking at its sequence, it is an extension of **LM2** with an additional 4 amino acids at the N-terminal and one at the C-terminal. As **LM2** gave good bioactivity, it is not surprising that **LM6** has even surpassed it. **LM6** has an additional positive charge, a higher hydrophobicity, and amphiphilicity. The second best, **LM9**, is a hybrid between **LM4** and **LM5**. It is a neutral peptide with low hydrophobicity, and high polar amino acid content. **LM9** was specifically chosen as it had some of the lowest scores for the AMP prediction. Nonetheless, it showed a very good activity profile against all Gram-positive pathogens, but with higher MIC values compared to **LM5** for the resistant strains, with 1.3 μM, 1.0 μM, 1.1 μM, 2.5 μM, and 3.1 μM against SA, *C. diff.*, Lm, MRSA, and VRE, respectively. **LM9** however remained inactive against the Gram-negative pathogens.

To verify whether the determined MIC kills the entire bacterial population, we performed the minimal bactericidal concentration (MBC) experiment for all tested peptides against all the pathogens. It showed that the peptides indeed killed the bacteria at the observed MIC values, as no bacterial growth was observed after 48 hours of incubation at 37 °C,

confirming that the MIC and MBC values were the same, and indicating a bactericidal mode of action.

Using this methodology, we were able to determine two main regions within the LM peptide that contribute most to the antibacterial activity, represented by the peptides **LM6** and **LM9**. Both peptides come from the second series obtained through AMP predictions. However, **LM9** and other peptides around that region had very low scores, probably because of the high proportion of polar amino acids, and would have been dismissed otherwise. Nonetheless, the other three AMP peptides with high AMP prediction scores all showed good MIC activities against the Gram-positive pathogens, including the resistant strains. Within the first series, the systemic splicing also led to the same general two regions with peptides **LM2** and **LM5**. More importantly, both methods were convergent in pinpointing the core region with antibacterial activity. We also evaluated the peptides for their anti-inflammatory activity based on the percentage reduction in multiple proinflammatory biomarkers' (IL-8, IL-6, IL-1B, and TNF-alpha) concentration in Caco-2 cell lines inoculated with the inflammatory-inducing pathogen *C. difficile* ATCC 43602. LM has shown excellent reduction in all four biomarkers, with 95% reduction in IL-8 concentration, 90% for IL6, 91% for IL-1B, and 80% for TNF alpha. This anti-inflammatory level of activity however could not be replicated in any of the shorter peptides. **LM4** showed some anti-inflammatory activity with 61% reduction in IL-8, 50% reduction in IL-6, and 19% reduction in IL-1B, while TNF alpha concentration was not affected. The **LM9** peptide, which contains part of **LM4**, reduced all four biomarkers IL-8, IL-6, IL-1B, and TNF-alpha by 12%, 32%, 33%, and 40%, respectively. **LM5**, on the other hand, which completes the C-terminal of the peptide, has induced a lower response with 18%, 12%, and 18% reduction of the respective interleukins, but none against TNF alpha. **LM7** also showed some moderate activity between 18 and 27% reduction of all four cytokines. **LM2**, **LM6**, and **LM8** induced the reduction of some cytokines by less than 20%, while **LM1** and **LM3** had virtually no effect. Despite not having a single peptide that has retained the full anti-inflammatory activity of the parent peptide, these results indicate that the C-terminal of the peptide is one of the key regions involved in the observed activity. Having a dual mode of action to target both the bacterial pathogen and the associated inflammation is of great interest in the development of novel therapeutics, specifically targeting complicated infections leading to sepsis.[30]

Follow-up series

After analysis of the obtained results, and the key regions identified within the peptide sequence, **LM6** was considered the best of the series, given its low micromolar MIC values against the Gram-positive pathogens and the resistant strains comparable to those of the parent peptide. But more importantly, it retained the Gram-negative activity against *E. coli* and showed new activity against Pa within the same range of the MIC as Lm. Three more peptides were considered by further truncating the sequence of **LM6**, given the activity profile of **LM2**. Two peptides, **LM10** and **LM11**, have ten amino acids including the lysine residue, compared to **LM2**, thus having a +2 charge. The third peptide is a hexamer of the N-terminal side of **LM6** with a charge of +2. **LM2** remained the best truncated derivative of **LM6**, as the other three also showed no activity against the tested resistant strains, nor the Gram-negative pathogens. **LM10** showed an MIC value of 2.4 μM against SA, similar to **LM2**, but higher MIC values against *C. diff.* and Lm. **LM11** showed activity exclusively against SA with a higher MIC of 5.1 μM. Surprisingly, the shorter **LM12** peptide still showed a moderate Gram-positive activity with MICs of 3.9 μM, 4.6 μM, and 5.1 μM against SA, *C. diff.* and Lm. The calculated physicochemical properties of the peptides differ slightly but are all within the same range or direction. As **LM6** remains the best performer peptide, we then synthesized and tested its macrocyclized derivatives. Cyclic peptides have been shown to have better stability *in vivo* in general, while sometimes being more active caused by a more rigid structure and fewer conformations in solution, facilitating their interaction with the biological target.[31–33] The macrocyclization reaction with PyBop gave two separable products (ML13a and ML13b), the major of which (**LM13a**) contains the epimerized valine residue at the C-terminal point of macrocyclization, as verified by Marfey's analysis (Table S2 and Fig. S2†).[34] No attempts were conducted at this stage to optimize the macrocyclization reaction and both macrocycles were tested. The presence of D-amino acids is another chemical strategy that is used to increase the stability of peptides.[35] Both cyclic peptides show mostly similar MIC values and a slight gain in activity compared to the linear peptide **LM6** against most pathogens tested, making them the best performers of this first round of design. The cytotoxicity of the best antibiotic compounds was evaluated against two human lung cancer cell lines H292 and A549. Although favourable *in silico* predictions were obtained, toxicity was observed and was more pronounced against the H292 cell line compared to A549. Despite the low therapeutic index of these peptides (ranging from 1 to 10 depending on the peptide and cell line), there is ample room for further improvement and proper optimization of these molecules. Decreasing the overall lipophilicity of the peptides and increasing the net positive charge and amphipathicity are strategies that have been previously successful in reducing the toxicity of AMP analogues.[36–38] More advanced modifications entail the introduction of peptoids, non-natural amino acids, and peptidomimetic scaffolds within the peptidic structure.[36,39–42]

Investigations into the mode of action. A preliminary study into the mode of action (MOA) of the most active peptide **LM6** and its cyclic derivative **LM13a** was conducted. First, a time-kill assay was undertaken to monitor the effect of the peptides on the growth of SA over time, in

comparison to amoxicillin (AMOX) as a positive control. **LM6**, **LM13a**, and the parent peptide LM have shown a rapid onset of action, with bactericidal activity against SA at their corresponding MIC concentration (Fig. 2A). While the untreated cells showed constant growth over time, AMOX and all tested peptides resulted in a significant reduction of bacterial growth (Fig. 2A). After 2 hours, AMOX resulted in a 4-log fold decrease in colony forming units or surviving bacteria, **LM13a** in 3-log fold decrease, and **LM6** and LM in 2-log fold decrease. **LM13a** reduced surviving bacteria by 5-log CFU mL^{-1} within 6 hours, while all the other molecules reached that level at the 12-hour mark, including AMOX. These results show the superiority of the cyclic derivative, exhibiting a faster bactericidal effect compared to the others. Additionally, transmission electron microscopy (TEM) was used to visualize ultrastructural changes to the cell membrane of SA in the presence of **LM6** and **LM13a** peptides. Most AMPs are known to have a membrane targeting MOA, where the interaction of the AMP with the cell-membrane components leads to membrane destabilization through the formation of pores and cavities resulting in leakage of intracellular components, cell lysis, and death.[25] Many of the SA cells treated with **LM6** showed clear deformation of the cells and complete disintegration and lysis of the bacterial cell wall, leading to fragmentation and leakage of the cell's intracellular content (Fig. 2C). Meanwhile some other cells demonstrated detachment of pieces of the cell wall. Treatment with the cyclic derivative **ML13a** also showed cell damage and extracellular protrusions that are most likely fragments of the lysed cell wall or leaked intracellular contents (Fig. 2D). Detached fragments were also seen, confirming the lytic effect on the cell wall.

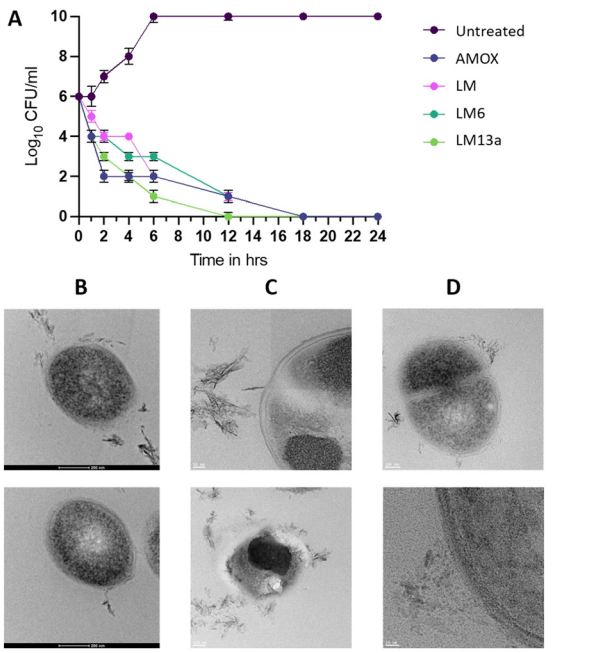

Fig. 2 Preliminary investigation into the possible mode of action of the designed peptide derivatives. A: Time-killing graph of *S. aureus* in the presence of the parent peptide LM, the best of series peptide LM6, its cyclic derivative LM13a, and the positive control antibiotic amoxicillin (Amox). B–D: TEM micrographs demonstrate the intact cell membrane of growing *S. aureus* cells (B) compared to a ruptured cell membrane (top) or complete disintegration and leakage (bottom) observed when the cells are treated with LM6 (C) and a partially disintegrated cell membrane with clear extracellular protrusions when cells are treated with the cyclic derivative LM13a (D).

Conclusions

Starting from lactomodulin, a 53-amino acid long peptide isolated from the gut microbiota with promising antibacterial and anti-inflammatory activities, we set out to determine the key core regions that would conserve the activity. As such, two series of nine peptides were determined based on systematic truncation of the parent peptide or AMP prediction calculations. The synthesized peptides ranging from 10–15 amino acid residues were evaluated for their antibacterial and anti-inflammatory activities. The two methods were convergent in identifying the best two regions within the peptide that conserved the antibacterial activity against Gram-positive pathogens and resistant strains spanning **LM2**/**LM6** and **LM5**/**LM9**. The Gram-negative activity against *E. coli* was conserved for **LM2** and **LM6**, in addition to the activity against *P. aeruginosa*. The anti-inflammatory activity however was very low for most peptides, with the best being peptides **LM4**, **LM7**, and **LM9**, showing anywhere between 18 and 61% reduction in some cytokine levels. The best of the series peptide **LM6** was further truncated, but the shorter peptides showed a significant decrease in activity. Finally, **LM6** was macrocyclized head-to-tail to generate two cyclic peptides **LM13a** and **LM13b**, where the former has an epimerized valine residue. The cyclic peptides proved to be the best performers, with similar or better activities against all the bacterial strains compared to **LM6**. The activity of LM6 and its cyclic derivatives against Gram-positive bacterial strains is comparable or superior to some commercial bactericidal antibiotics tested in this study. The best six antibacterial peptides were assessed against two human cancer cell lines but showed toxicity and low therapeutic index. Further optimization in the next round of design to improve the peptides' properties is considered. The **LM6** and **LM13a** peptides were found to be bactericidal at their MIC concentration using a time-kill curve and were shown to have a membrane-targeting mode of action by transmission electron microscopy. Bacterial cells of *S. aureus* treated with either of the compounds have shown clear signs of membrane damage and intracellular content leakage. This study has identified **LM6** as an ideal starting point for the generation of lactomodulin-inspired antibacterial peptides through further optimizations. Despite not having a conserved anti-inflammatory activity, other regions within the peptide have shown promise for the development of peptides with dual antibacterial and anti-inflammatory

activities. Further investigations around the optimization of the identified peptides and a detailed study of their antibacterial properties and mechanism of action, as well as their potential for selecting resistance are currently underway.

Experimental

Materials and methods

Bacterial strains. The bacterial strains *S. aureus* ATCC 25923, *C. difficile* ATCC 43602, *L. monocytogenes* ATCC 15313, *S. aureus* MRSA BAA 2313, *E. faecium* VRE BAA 2317, *E. coli* ATCC 33694, *P. aeruginosa* BAA 1744, and *S. enterica* ATCC 13314 were obtained from the American Type Culture Collection.

Cell lines. The cell lines A549 (catalog #86012804), H292 (catalog #91091815), and Caco-2 (catalog #86010202) were procured from Sigma-Aldrich, USA. The A549 and H292 cells were cultured in RPMI-1640 medium (catalog #R8758), while the Caco-2 cells were grown in DMEM (catalog #D6429). Both media were supplemented with 10% fetal bovine serum (catalog #F9665) and antibiotics (catalog #A5955), consisting of 100 U ml^{-1} penicillin and 100 μg ml^{-1} streptomycin. Cultures were maintained in a humidified incubator at 37 °C with 5% CO_2.

Chemicals and reagents. Fmoc-Rink Amide aminomethyl-polystyrene resin, 2-chlorotrityl chloride (2-CTC) resin, was obtained from Hecheng (China). HBTU, ethyl (hydroxyimino) cyanoacetate (OxymaPure®), and Fmoc-protected amino acids were obtained from Iris Biotech (Germany). Triisopropyl silane (TIS), *N*,*N*′-diisopropylcarbodiimide (DIC), DIPEA, TIPS, piperidine, and *N*,*N*-dimethylformamide (DMF) were purchased from Merck (Germany) or Sigma-Aldrich (Germany). TFA was procured from Iris Biotech (Germany) or Sigma-Aldrich (Germany). Dichloromethane, diethyl ether, LCMS grade and HPLC grade acetonitrile were purchased from Honeywell (Germany). Amoxycillin, fidaxomicin, and ciprofloxacin were purchased from Merck (Germany). All chemicals and solvents were used without any further purification. The LM peptide was purchased from Genscript Inc. (Piscataway, NJ, USA). Water used for analytical and preparative high-performance liquid chromatography (HPLC) was filtered (0.22 μm) in-house using a Q-POD® ultrapure water remote dispenser connected to a Milli-Q® IQ water system.

General procedures. Analytical HPLC was performed on an Agilent® Eclipse Plus C18 column (150 mm × 4.6 mm; particle size: 5 μm; pore size: 95 Å) using a Thermo Scientific Ultimate 3000 system, eluting using a linear gradient over 25 minutes with H_2O and acetonitrile (MeCN) with 0.1% trifluoroacetic acid (TFA) added to the eluents, going from 0 to 50% MeCN with UV detection at λ = 220 nm and coupled to a Q Exactive mass spectrometer with HRMS and MS^2 capability. Preparative HPLC was performed by using an Agilent InfinityLab ZORBAX 5 SB-C18 column (250 × 21.2 mm; particle size: 5 μm; pore size 80 Å) on an Ultimate 3000 system using the same eluents as for analytical HPLC. High-resolution mass spectrometry (HRMS) and MS/MS spectra were obtained simultaneously on a Thermo Scientific 3000 ultimate HPLC coupled with a Q Exactive mass spectrometer using both full scan and MS/MS in the positive mode (full MS: sheath gas flow rate 50, aux gas flow rate 13, polarity positive, spray voltage 3.5 kV, capillary temperature 263 C, aux gas temperature 425, resolution 70 000).

Synthesis of linear peptides. All the peptides were synthesized by a solid-phase method using the Fmoc/*t*Bu strategy on a Syro wave I (Biotage, Sweden) automated peptide synthesizer. All the linear peptides are amidated at the C-terminal, through the use of the rink amide resin. The synthesis employed the standard coupling/deprotection protocol and final cleavage. For all peptides **LM1–LM12**, the same general synthetic strategy was followed. First, the rink amide resin (78 mg, 0.53 mmol g^{-1} loading, 100–200 mesh) was swelled in 1 : 1 DMF : DCM for 5 min before use and then washed with DMF. Fmoc-protected amino acid building block (5.0 equiv.) coupling was performed using a double coupling strategy at room temperature for 0.5 h each coupling with intermittent shaking every 2 min. The first coupling uses DIC (0.5 M in DMF; 5.0 equiv.) and OxymaPure® (2.0 M in DMF; 5.0 equiv.) and the second uses HBTU (0.48 M in DMF; 5.0 equiv.) and DIPEA (2 M in NMP; 5.0 equiv.). Fmoc deprotection was performed in two steps with 40% (v/v) piperidine in DMF at rt for 3 min and 20% (v/v) piperidine in DMF at rt for 9 min, with shaking, followed by washing with DMF. Cleavage was performed off-line by treating the resin-bound peptide with 2 mL of a TFA/H_2O/TIPS mixture (95 : 2.5 : 2.5; v/v) two times for 1 h each. The combined eluates were kept at rt for 2–3 h. The solution was transferred into a round-bottom flask and co-evaporated with toluene. The addition of cold diethyl ether resulted in the precipitation of the crude peptide. Crude peptides were purified by semi-preparative RP-HPLC using a linear gradient of 0–40% ACN over 20 min with a flow rate of 20 mL min^{-1}. The purity and identity of the peptides were verified by analytical HPLC and LC-MS HRMS analysis, respectively. The purified peptides were freeze-dried and stored at −20 °C until biological testing.

Synthesis of macrocyclic peptides. The macrocyclic peptide **LM13** was synthesized on a 2-CTC resin and the macrocyclization took place in solution on the crude peptide before deprotection. First, the 2-CTC resin (78 mg, 0.53 mmol g^{-1} loading, 100–200 mesh) was swelled in 10% DIPEA in dry DCM for 10 min before use and then washed with dry DCM and drained. Fmoc-Val-OH (5 equiv.) and DIPEA (10 equiv.) dissolved in 1 mL of dry DCM were added to the resin. The reaction was kept shaking for 3 h at room temperature under inert atmosphere. After draining, the resin was washed and drained three times with DMF, DCM, and DMF successively and then capped with a 0.5 mL solution of MeOH/DIPEA (1 : 2) in DCM (3 mL) to quench unreacted CTC for 0.5 h at rt. After washing, the initial linear peptide was then completed on the automated Syro I

(Biotage) peptide synthesizer. The procedure for coupling/deprotection cycles is the same as the one described for the other linear peptides. After complete synthesis, the resin was washed with two cycles of successive DMF and DCM washing. Full cleavage of the side-chain fully-protected peptide was achieved by adding 30% HFIP in DCM and shaking at room temperature over 1 h. The crude peptide (80 mg) was obtained after evaporation and was directly used for the cyclization reaction. The crude peptide was dissolved in 40 mL DMF, and DIPEA (50 μL, 6 equiv.) was added to the solution. Then PyBOP (80 mg, 3 equiv.) was added and the reaction mixture stirred overnight at rt. Progress of the macrocyclization reaction was monitored by LCMS. DMF was removed under reduced pressure and the crude macrocyclic peptide was obtained by addition of 20 mL MeCN : H_2O (1 : 1) followed by centrifugation. The final deprotection was then done by treating the crude macrocycle with the TFA/H_2O (97.5 : 2.5) solution for 3 h while shaking. Progress of the deprotection was also monitored by LCMS. TFA was co-evaporated with toluene and cold diethyl ether was added to precipitate the peptide. The crude was then purified by semi-preparative RP-HPLC using a linear gradient of 0–100% MeCN over 25 min with a flow rate of 20 mL min^{-1}. Two macrocyclic products, **LM13a** (major) and **LM13b** (minor), with the same mass were observed and separated. The purified peptides were freeze-dried and stored at −20 °C until biological testing.

All the peptides had a purity >95%, except for **LM1** at 76% after two purification rounds. Total yields of the linear peptides were approximately 10–38% based on the resin loading (for each compound, the yield is stated in Table S1†). The analytical reversed-phase HPLC chromatograms and ESI mass spectra for purified peptides are presented in Fig. S2–S15.†

Marfey's analysis. The absolute configuration of the valine residues within the cyclic peptides **LM13a** and **LM13b** was determined by Marfey's method.[43] About 200 μg of each peptide and an L-Val standard were dissolved in 6 M HCl (100 μL) and heated to 110 °C for 45 min and then dried at 110 °C in 15 min. To the dried samples, H_2O (50 μL) and 1 M $NaHCO_3$ (200 μL) were added, and then divided into two equal portions. The Marfey's solutions were prepared with 5 mg of Marfey's reagent diluted in acetone (2 mL). A 100 μL aliquot of Marfey's solution (L- and D-FDLA) was added to the two corresponding portions of each sample, respectively. The vials were heated to 40 °C for 1 h, then quenched with 200 μL of 1 M HCl. Finally, the reaction products were diluted with MeCN (200 μL) and filtered prior to LC-MS analysis. Aliquots (10 μL) of each sample were then injected to LC-MS for analysis. The optimized acidic pH solvent system consisted of solvent A (H_2O/0.1% TFA) and solvent B (MeCN/0.1% TFA). The optimized gradient was 5–10% B (0–1 min), 10–35% B (1–14 min), 35–55% B (14–21 min), 55–80% B (21–24 min), and 80% B (24–25 min) at 45 °C, flow 0.6 mL min^{-1} and UV at 340 nm. MS detection was done using the negative ion mode and corresponding masses extracted from the full scan.

Agar diffusion test. In summary, a 10 μL aliquot of actively growing overnight culture for each pathogen was spread onto agar plates. Subsequently, sterile glass pipettes were used to puncture holes in the agar, into which 20 μL of peptides ranging from 1 to 10 μM concentration were added. The plates were then aerobically incubated at 37 °C for 24 hours. Following incubation, the plates were examined to detect any zones of inhibition.

Minimal inhibitory concentration (MIC). To determine the MIC of each peptide against the tested pathogens, a broth microdilution antimicrobial assay was performed using a 96-well microtiter plate.[44] A single colony of each pathogen was cultured for 24 hours in its recommended broth medium under its optimum growth conditions, then diluted with the same medium in a 1 : 10 000 ratio, following the McFarland Standards. Subsequently, 196 μL of this inoculated medium was dispensed into each well, followed by the addition of 4 μL of various serial dilutions of each peptide into the respective wells. The control wells were filled with 196 μL of non-inoculated medium and 4 μL of DMSO, the solvent used to dissolve the peptides. Fidaxomicin, amoxicillin, and ciprofloxacin served as positive controls. Plates were then incubated aerobically or anaerobically, depending on the growth requirements of each pathogen, at 37 °C. Following a 24-hour incubation period, the OD_{600} of each well was measured using a microplate reader. Subsequently, the MIC, defined as the lowest peptide concentration resulting in 100% growth inhibition, was determined for each pathogen. Each concentration was tested in duplicate, and the entire assay was independently repeated five times. The percentage of growth inhibition was calculated using the following equation:

$$\%\ \text{of inhibition} = 1 - [(OD_{600}\ \text{test} - OD_{600}\ \text{blank medium})/(OD_{600}\ \text{pathogen only} - OD_{600}\ \text{blank medium})] \times 100$$

Minimal bactericidal concentration (MBC). To verify that the determined MIC kills the entire bacterial population, we dispensed 10 μL of the inhibitory concentrations identified from the broth microdilution assay (where no growth was detected) onto agar plates. These plates were then incubated for 48 hours at 37 °C, after which we examined them for the presence of any colonies. Control experiments included a culture treated with fidaxomicin at a concentration of 1 μM.

Anti-inflammatory activity. To evaluate the potential anti-inflammatory properties of the synthesized peptides, a cell-based assay was conducted using human colorectal adenocarcinoma Caco-2 cells following a standard protocol.[14] These cells were cultured in Dulbecco's modified Eagle's medium (DMEM) supplemented with 10% fetal bovine serum at 37 °C in an environment containing 5% CO_2 (Eppendorf, Hamburg, Germany). Cultures were maintained until cells

reached 90% confluence over a 5-day period. Subsequently, PBS buffer was used to wash the cells 2–3 times to remove culture media or non-adherent cells. Prior to each assay, cells were seeded into 12-well tissue-culture plates (BD Falcon, Becton, NJ, USA) and incubated for 24 hours in a 5% CO_2 incubator at 37 °C, with a seeding density of 30 000 cells per well. Overall, the experimental design involved treatment of the cell lines challenged with an inflammation-inducing pathogen with each peptide then measurement of the released pro-inflammatory cytokines in the culture supernatant using commercially available ELISA kits. The pathogen *C. difficile* was used as a model to induce inflammation. Briefly, *C difficile* was cultured overnight in meat broth medium at 37 °C under anaerobic conditions. The culture was then subjected to centrifugation at 12 000 × *g* for 2 minutes, followed by two washes with PBS buffer and suspension in meat broth. Subsequently, 1 μL of 0.5 OD_{600} culture was used for each 300 μL of culture medium in every well of the 12-well plate. After a 2-hour incubation period, 1 μL of each peptide was added to achieve a final concentration equivalent to the MIC. Negative control experiments included untreated cells or cells treated with DMSO, while positive controls consisted of cells treated with the pathogen only. The duration of incubation was determined through prior optimization experiments and referenced from previous reports regarding the optimal timing for cytokine release and measurement in Caco-2 cells. To quantify cytokine release in Caco-2 cells following co-incubation, an enzyme-linked immunosorbent assay (ELISA) was employed for IL8, IL-6, IL-1β, and TNF-α in the collected supernatant. Commercial kits from Invitrogen, Carlsbad, CA, USA (catalog numbers BMS204-3, BMS213HS, KHC001, and BMS223-4 for IL8, IL-6, IL-1β, and TNFα, respectively) were utilized for this purpose. Cytokine levels were determined following the provided protocol. Each analysis was conducted in three independent replicates.

Cell viability and proliferation assay. To evaluate the cytotoxic effects of the synthesized peptides, an MTT (3-[4,5-dimethylthiazol-2-yl]-2,5-diphenyl tetrazolium bromide) assay was employed on two lung cancer cell lines, namely A549 and H292.[45] These cell lines were cultured in RPMI-1640 medium (#R8758, Sigma, USA), supplemented with 10% fetal bovine serum and antibiotics (100 U ml^{-1} penicillin and 100 μg ml^{-1} streptomycin), within a humidified incubator (5% CO_2 in air at 37 °C). Each cell line was seeded in 96-well plates at a density of 30 000 cells per well (200 μL per well), treated with a serial dilution of each peptide at concentrations of 50 μM, 10 μM, 1 μM, 0.1 μM, and 0.01 μM, and incubated in a CO_2 incubator for 24 hours. Following the removal of the supernatant and washing twice with PBS1X, 20 μL of MTT solution was added to each well and incubated for 3 hours. Subsequently, the absorbance intensity was measured using spectrophotometry with a microplate reader at an absorbance wavelength of 570 nm (Thermo Fisher Scientific, Waltham, MA, USA). DMSO was used as the negative control. EC_{50} values were calculated using OD values (triplicate) normalized to blank (average of six) and an online software program (AAT Bioquest EC50 Calculator).[46]

Time-kill kinetic assay. Time-kill curves were used to monitor bacterial growth over time.[47] First, *S. aureus* (ATCC 25923) was grown overnight on TSA plates at 37 °C, then diluted to a working concentration of 5×10^5 CFU ml^{-1} using Mueller–Hinton broth (Oxoid, United Kingdom). Thereafter, the test compounds were added to the bacteria, at the MIC concentration, in a 96-well plate format. Aliquots were taken at different time points (0, 1, 2, 4, 6, 12, 18, and 24 h). At every time interval, a 5 μl sample was taken from each well, serially diluted tenfold in a solution of 0.85% NaCl, plated on TSA, and incubated overnight at 37 °C. Colony forming units (CFUs) were calculated and the experiment was repeated in two independent duplicates.

TEM characterization. TEM imaging was conducted to visualize any change in the cell morphology or cell membrane upon treatment with the synthesized peptides.[48] Initially, a single colony from an overnight culture was suspended in 10 ml of LB broth and incubated with continuous shaking at 37 °C overnight. The overnight culture was diluted (1 : 30) in 40 ml of LB broth and shaken continuously for 2 hours until the OD_{600} reached approximately 0.5. Subsequently, the tested compounds were added at their minimum inhibitory concentration (MIC) and incubated at 37 °C. Cells were then centrifuged at 4 °C to prevent cell damage, followed by washing and resuspension in 0.1 M phosphate-buffered saline (PBS; pH 7.2). The fixed cells were preserved overnight using a fixative solution comprising 4% formaldehyde, 1.25% glutaraldehyde, 4% sucrose, 0.01 M $CaCl_2$, and 0.075% ruthenium red in PBS. Following preservation, the fixed cells underwent a series of washes in PBS buffer and were post-fixed for 1 hour with 1% osmium tetroxide in PBS supplemented with 0.075% ruthenium red, followed by further washing. Dehydration was achieved through successive ethanol treatments (30%, 50%, 70%, 80%, 90%, 95%, and 100%), each lasting 15 minutes, ultimately culminating in treatment with propylene oxide. The cells were then infiltrated with a mixture of propylene oxide and Agar 100 epoxy resin in ratios of 1 : 1, 1 : 2, and 1 : 3, and subsequently polymerized at 65 °C for 24 hours. The resulting blocks were trimmed, and ultrathin sections (95 nm) with gold coloration were cut using an EM UC7 Ultracuts ultramicrotome from Leica (Vienna, Austria). Ultrathin sections were collected on 200 mesh copper grids, air-dried, and then contrasted with uranyl acetate and lead citrate. The grids were subsequently examined using a transmission electron microscope, with images captured at varying magnifications using the Titan system at 300 kV. The entire experiment was repeated in duplicate.

Data availability

The data supporting this article have been included as part of the ESI.†

Author contributions

E. O. and W. M. conceptualized, designed, directed, supervised, acquired funding, and coordinated the study. A. S. and M. A. performed the synthesis, purification, and analysis of the peptides; W. M. conducted the time-kill and ELISA assays; W. M. and A. A. conducted the antimicrobial assays; R. G., N. S. and M. K. conducted, and analysed data for cell-line based assays; F. A. and W. M. prepared the TEM samples and M. I. H. ran the TEM experiments; F. A. analysed the TEM results; E. O. and W. M. wrote the original draft. All authors contributed to editing and revising and have given approval to the final version of the manuscript.

Conflicts of interest

There are no conflicts to declare.

Acknowledgements

The authors are grateful for the financial support provided by Khalifa University of Science and Technology for starting grant to E. O. (FSU-2022-019) and internal grant from Al Ain University to W. M. (Ph2023-4-103). The authors would like to thank Mr. Mohan Rommala from the ACBC core lab at KU.

Notes and references

1 H. Fongang, A. T. Mbaveng and V. Kuete, in *Advances in Botanical Research*, Elsevier, 2023, vol. 106, pp. 1–20.
2 C. J. L. Murray, K. S. Ikuta, F. Sharara, L. Swetschinski, G. Robles Aguilar, A. Gray, C. Han, C. Bisignano, P. Rao, E. Wool, S. C. Johnson, A. J. Browne, M. G. Chipeta, F. Fell, S. Hackett, G. Haines-Woodhouse, B. H. K. Hamadani, E. A. P. Kumaran, B. McManigal, S. Achalapong, R. Agarwal, S. Akech, S. Albertson, J. Amuasi, J. Andrews, A. Aravkin, E. Ashley, F.-X. Babin, F. Bailey, S. Baker, B. Basnyat, A. Bekker, R. Bender, J. A. Berkley, A. Bethou, J. Bielicki, S. Boonkasidecha, J. Bukosia, C. Carvalheiro, C. Castañeda-Orjuela, V. Chansamouth, S. Chaurasia, S. Chiurchiù, F. Chowdhury, R. Clotaire Donatien, A. J. Cook, B. Cooper, T. R. Cressey, E. Criollo-Mora, M. Cunningham, S. Darboe, N. P. J. Day, M. De Luca, K. Dokova, A. Dramowski, S. J. Dunachie, T. Duong Bich, T. Eckmanns, D. Eibach, A. Emami, N. Feasey, N. Fisher-Pearson, K. Forrest, C. Garcia, D. Garrett, P. Gastmeier, A. Z. Giref, R. C. Greer, V. Gupta, S. Haller, A. Haselbeck, S. I. Hay, M. Holm, S. Hopkins, Y. Hsia, K. C. Iregbu, J. Jacobs, D. Jarovsky, F. Javanmardi, A. W. J. Jenney, M. Khorana, S. Khusuwan, N. Kissoon, E. Kobeissi, T. Kostyanev, F. Krapp, R. Krumkamp, A. Kumar, H. H. Kyu, C. Lim, K. Lim, D. Limmathurotsakul, M. J. Loftus, M. Lunn, J. Ma, A. Manoharan, F. Marks, J. May, M. Mayxay, N. Mturi, T. Munera-Huertas, P. Musicha, L. A. Musila, M. M. Mussi-Pinhata, R. N. Naidu, T. Nakamura, R. Nanavati, S. Nangia, P. Newton, C. Ngoun, A. Novotney, D. Nwakanma, C. W. Obiero, T. J. Ochoa, A. Olivas-Martinez, P. Olliaro, E. Ooko, E. Ortiz-Brizuela, P. Ounchanum, G. D. Pak, J. L. Paredes, A. Y. Peleg, C. Perrone, T. Phe, K. Phommasone, N. Plakkal, A. Ponce-de-Leon, M. Raad, T. Ramdin, S. Rattanavong, A. Riddell, T. Roberts, J. V. Robotham, A. Roca, V. D. Rosenthal, K. E. Rudd, N. Russell, H. S. Sader, W. Saengchan, J. Schnall, J. A. G. Scott, S. Seekaew, M. Sharland, M. Shivamallappa, J. Sifuentes-Osornio, A. J. Simpson, N. Steenkeste, A. J. Stewardson, T. Stoeva, N. Tasak, A. Thaiprakong, G. Thwaites, C. Tigoi, C. Turner, P. Turner, H. R. Van Doorn, S. Velaphi, A. Vongpradith, M. Vongsouvath, H. Vu, T. Walsh, J. L. Walson, S. Waner, T. Wangrangsimakul, P. Wannapinij, T. Wozniak, T. E. M. W. Young Sharma, K. C. Yu, P. Zheng, B. Sartorius, A. D. Lopez, A. Stergachis, C. Moore, C. Dolecek and M. Naghavi, *Lancet*, 2022, **399**, 629–655.
3 G. S. Tillotson and S. H. Zinner, *Expert Rev. Anti-infect. Ther.*, 2017, **15**, 663–676.
4 M. S. Donia, P. Cimermancic, C. J. Schulze, L. C. Wieland Brown, J. Martin, M. Mitreva, J. Clardy, R. G. Linington and M. A. Fischbach, *Cell*, 2014, **158**, 1402–1414.
5 C. D. Santos-Júnior, M. D. T. Torres, Y. Duan, Á. Rodríguez Del Río, T. S. B. Schmidt, H. Chong, A. Fullam, M. Kuhn, C. Zhu, A. Houseman, J. Somborski, A. Vines, X.-M. Zhao, P. Bork, J. Huerta-Cepas, C. De La Fuente-Nunez and L. P. Coelho, *Cell*, 2024, **187**, 3761–3778.
6 M. R. Wilson, L. Zha and E. P. Balskus, *J. Biol. Chem.*, 2017, **292**, 8546–8552.
7 H.-Y. Cheng, M.-X. Ning, D.-K. Chen and W.-T. Ma, *Front. Immunol.*, 2019, **10**, 607.
8 K. Hou, Z.-X. Wu, X.-Y. Chen, J.-Q. Wang, D. Zhang, C. Xiao, D. Zhu, J. B. Koya, L. Wei, J. Li and Z.-S. Chen, *Signal Transduction Targeted Ther.*, 2022, **7**, 135.
9 M. Mahlapuu, J. Håkansson, L. Ringstad and C. Björn, *Front. Cell. Infect. Microbiol.*, 2016, **6**, 194.
10 J. Xuan, W. Feng, J. Wang, R. Wang, B. Zhang, L. Bo, Z.-S. Chen, H. Yang and L. Sun, *Drug Resistance Updates*, 2023, **68**, 100954.
11 H. B. Koo and J. Seo, *Pept. Sci.*, 2019, **111**, e24122.
12 G. S. Dijksteel, M. M. W. Ulrich, E. Middelkoop and B. K. H. L. Boekema, *Front. Microbiol.*, 2021, **12**, 616979.
13 L. Gallardo-Becerra, M. Cervantes-Echeverría, F. Cornejo-Granados, L. E. Vazquez-Morado and A. Ochoa-Leyva, *Microb. Ecol.*, 2024, **87**, 8.
14 W. K. Mousa, R. Ghemrawi, T. Abu-Izneid, A. Ramadan and F. Al-Marzooq, *IJMS*, 2023, **24**, 6901.
15 F. H. Waghu, R. S. Barai, P. Gurung and S. Idicula-Thomas, *Nucleic Acids Res.*, 2016, **44**, D1094–D1097.
16 M. N. Gabere and W. S. Noble, *Bioinformatics*, 2017, **33**, 1921–1929.
17 S. Gupta, P. Kapoor, K. Chaudhary, A. Gautam, R. Kumar, Open Source Drug Discovery Consortium and G. P. S. Raghava, *PLoS One*, 2013, **8**, e73957.
18 M. Baek, F. DiMaio, I. Anishchenko, J. Dauparas, S. Ovchinnikov, G. R. Lee, J. Wang, Q. Cong, L. N. Kinch, R. D. Schaeffer, C. Millán, H. Park, C. Adams, C. R. Glassman, A. DeGiovanni, J. H. Pereira, A. V. Rodrigues, A. A. van Dijk,

A. C. Ebrecht, D. J. Opperman, T. Sagmeister, C. Buhlheller, T. Pavkov-Keller, M. K. Rathinaswamy, U. Dalwadi, C. K. Yip, J. E. Burke, K. C. Garcia, N. V. Grishin, P. D. Adams, R. J. Read and D. Baker, *Science*, 2021, **373**, 871–876.

19 M. Baek, I. Anishchenko, I. R. Humphreys, Q. Cong, D. Baker and F. DiMaio, *bioRxiv*, 2023, preprint, DOI: **10.1101/2023.05.24.542179**.

20 D. Xu and Y. Zhang, *Proteins*, 2012, **80**, 1715–1735.

21 S. M. Mortuza, W. Zheng, C. Zhang, Y. Li, R. Pearce and Y. Zhang, *Nat. Commun.*, 2021, **12**, 5011.

22 A. Lamiable, P. Thévenet, J. Rey, M. Vavrusa, P. Derreumaux and P. Tufféry, *Nucleic Acids Res.*, 2016, **44**, W449–W454.

23 M. Pirtskhalava, A. A. Amstrong, M. Grigolava, M. Chubinidze, E. Alimbarashvili, B. Vishnepolsky, A. Gabrielian, A. Rosenthal, D. E. Hurt and M. Tartakovsky, *Nucleic Acids Res.*, 2021, **49**, D288–D297.

24 D. Eisenberg, R. M. Weiss, T. C. Terwilliger and W. Wilcox, *Faraday Symp. Chem. Soc.*, 1982, **17**, 109.

25 Q.-Y. Zhang, Z.-B. Yan, Y.-M. Meng, X.-Y. Hong, G. Shao, J.-J. Ma, X.-R. Cheng, J. Liu, J. Kang and C.-Y. Fu, *Mil. Med. Res.*, 2021, **8**, 48.

26 Y. Chen, M. T. Guarnieri, A. I. Vasil, M. L. Vasil, C. T. Mant and R. S. Hodges, *Antimicrob. Agents Chemother.*, 2007, **51**, 1398–1406.

27 I. A. Edwards, A. G. Elliott, A. M. Kavanagh, J. Zuegg, M. A. T. Blaskovich and M. A. Cooper, *ACS Infect. Dis.*, 2016, **2**, 442–450.

28 S. Mitaku, T. Hirokawa and T. Tsuji, *Bioinformatics*, 2002, **18**, 608–616.

29 K. L. Zapadka, F. J. Becher, A. L. Gomes Dos Santos and S. E. Jackson, *Interface Focus*, 2017, **7**, 20170030.

30 Y. Acharya, K. K. Taneja and J. Haldar, *RSC Med. Chem.*, 2023, **14**, 1410–1428.

31 H. Huang, J. Damjanovic, J. Miao and Y.-S. Lin, *Phys. Chem. Chem. Phys.*, 2021, **23**, 607–616.

32 X. Ji, A. L. Nielsen and C. Heinis, *Angew. Chem.*, 2024, **136**, e202308251.

33 E. Oueis, T. Klefisch, N. Zaburannyi, R. Garcia, A. Plaza and R. Müller, *Org. Lett.*, 2019, **21**, 5407–5412.

34 C. Bechtler and C. Lamers, *RSC Med. Chem.*, 2021, **12**, 1325–1351.

35 Z. Y. Ong, N. Wiradharma and Y. Y. Yang, *Adv. Drug Delivery Rev.*, 2014, **78**, 28–45.

36 A. A. Robles-Loaiza, E. A. Pinos-Tamayo, B. Mendes, J. A. Ortega-Pila, C. Proaño-Bolaños, F. Plisson, C. Teixeira, P. Gomes and J. R. Almeida, *Pharmaceuticals*, 2022, **15**, 323.

37 Y. Lyu, Y. Yang, X. Lyu, N. Dong and A. Shan, *Sci. Rep.*, 2016, **6**, 27258.

38 A. Hawrani, R. A. Howe, T. R. Walsh and C. E. Dempsey, *J. Biol. Chem.*, 2008, **283**, 18636–18645.

39 S. Jaber, V. Nemska, I. Iliev, E. Ivanova, T. Foteva, N. Georgieva, I. Givechev, E. Naydenova, V. Karadjova and D. Danalev, *Molecules*, 2021, **26**, 7321.

40 G. N. Enninful, R. Kuppusamy, E. K. Tiburu, N. Kumar and M. D. P. Willcox, *J. Pept. Sci.*, 2024, **30**, e3560.

41 Y. M. Song, Y. Park, S. S. Lim, S.-T. Yang, E.-R. Woo, I.-S. Park, J. S. Lee, J. I. Kim, K.-S. Hahm, Y. Kim and S. Y. Shin, *Biochemistry*, 2005, **44**, 12094–12106.

42 W. L. Zhu, K. Hahm and S. Y. Shin, *J. Pept. Sci.*, 2007, **13**, 529–535.

43 B. Zhou, G. Shetye, N. M. Wolf, S.-N. Chen, M. Qader, G. J. Ray, D. C. Lankin, S. Cho, J. Cheng, J.-W. Suh, S. G. Franzblau, J. B. McAlpine and G. F. Pauli, *Org. Lett.*, 2022, **24**, 7265–7270.

44 P. Parvekar, J. Palaskar, S. Metgud, R. Maria and S. Dutta, *Biomater. Invest. Dent.*, 2020, **7**, 105–109.

45 M. Ghasemi, T. Turnbull, S. Sebastian and I. Kempson, *IJMS*, 2021, **22**, 12827.

46 AAT Bioquest., AAT Bioquest, Inc., **https://www.aatbio.com/tools/ec50-calculator**, (accessed 30 April 2024).

47 E. B. A. Adusei, R. K. Adosraku, J. Oppong-Kyekyeku, C. D. K. Amengor and Y. Jibira, *J. Trop. Med.*, 2019, **2019**, 1–8.

48 J. Zahller and P. S. Stewart, *Antimicrob. Agents Chemother.*, 2002, **46**, 2679–2683.